Journal of Materials Chemistry B

ROYAL SOCIETY OF CHEMISTRY

PAPER

View Article Online
View Journal | View Issue

Check for updates

Cite this: J. Mater. Chem. B, 2023, 11, 3816

The memory effect of micro/nano-structures activating osteogenic differentiation of BMSCs

Cancan Zhao,†[ab] Chen Yang,†[cd] Qun Lou,[b] Jiashu Yan,[b] Xudong Wang*[b] and Jiang Chang*[acd]

Received 16th February 2023,
Accepted 3rd April 2023

DOI: 10.1039/d3tb00337j

rsc.li/materials-b

Degradable bioceramics such as hydroxyapatite (HA) are usually used as bone grafts due to their excellent osteoconductive ability. Recent studies have proved that decorated micro/nano-structures on HA could enhance its osteogenic capacity by directly activating osteogenic differentiation of bone marrow-derived stem cells (BMSCs) or by indirectly activating the osteoimmune microenvironment. However, it is still unclear whether the degradation process of HA affects the activation effect of micro/nano-structures. In this study, we first demonstrate that the enhanced osteogenic properties activated by micro/nano-structures could be memorized and continue to play a role even after the removal of micro/nano-structures. More interestingly, this topography-triggered osteogenic memory effect (TTOME) could be regulated through the stimulation time, indicating the importance of the rational maintenance of micro/nano-structures as well as the degradation process of bioceramics. These findings provide a perspective of the design of bone implants with a biodegradable surface topography.

1. Introduction

Bone defect is a common clinical disease that usually requires bone grafts to serve as a bridge for the defect site and guide the growth of newly formed bone tissue.[1–4] An ideal bone graft usually possesses an optimal architecture including the framework, porous structure, and surface topography, especially for surface topography, and directly interacts with the host body after implantation.[5,6] Recent studies have shown that micro/nano-structured surface topography plays a key role in stimulating bone regeneration.[7,8] For example, the micropatterns on hydroxyapatite (HA) with different sizes are able to stimulate osteogenic differentiation of bone marrow-derived stem cells (BMSCs), especially for micropatterns with the size similar to the diameter of BMSCs.[9] Interestingly, Ma *et al.*[10] also found that nanostructures obtained through alkali heat treatment could stimulate the secretion of small extracellular vesicles from BMSCs to further promote osteogenesis through miRNA. In addition to the direct regulation of bone-forming cells, the osteoimmunomodulation regulated by the bone implant is also critical, which usually determines the ultimate success of the implants through the interaction with immune cells.[11,12] It has been found that suitable surface topographies of biomaterials can modulate the immune response, and further enhance bone regeneration by profitable osteoimmunomodulation.[13–15] For example, titanium-based implants with nanotubes effectively induced macrophage polarization towards the healing-associated M2 phenotype, and supported the formation of a new bone tissue.[16,17] Our previous studies also demonstrated that the micro/nano-hierarchical structure of HA could significantly activate macrophages by converting M1/M2 polarization for osteoimmunomodulation as compared to the pure nano- or micro-structure.[18]

However, these micro- or nano-surface structures are not permanent *in vivo* due to their biodegradability. It is unknown whether the micro/nano-structure activated osteogenic properties are retained when the micro/nano-structures are degraded during the degradation process of bioceramics. Also, if the topography-triggered osteo-relative properties can be remembered, can it be regulated by the stimulation time? To better answer this question, we utilized HA with different micro or nano-structures as a bone graft model for cell study since its degradation rate is extremely low *in vitro*, which guarantees the

[a] State Key Laboratory of High Performance Ceramics and Superfine Microstructure, Shanghai Institute of Ceramics, Chinese Academy of Sciences, Shanghai 200050, P. R. China. E-mail: jchang@mail.sic.ac.cn
[b] Department of Oral & Cranio-Maxillofacial Surgery, Shanghai Ninth People's Hospital, Shanghai Jiao Tong University School of Medicine; College of Stomatology, Shanghai Jiao Tong University, National Center for Stomatology, National Clinical Research Center for Oral Diseases, Shanghai Key Laboratory of Stomatology, Shanghai Research Institute of Stomatology, Shanghai 200011, P. R. China. E-mail: xudongwang70@hotmail.com
[c] Joint Centre of Translational Medicine, the First Affiliated Hospital of Wenzhou Medical University, Wenzhou 325000, China
[d] Zhejiang Engineering Research Center for Tissue Repair Materials, Wenzhou Institute, University of Chinese Academy of Sciences, Wenzhou 325000, China
† These authors contributed equally to this work.

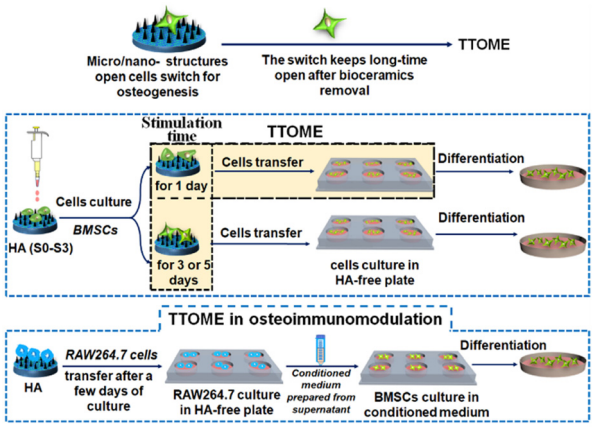

Scheme 1 Schematic illustration of the TTOME on BMSCs.

stability of the existing topographies and makes the investigation of tailored stimulation time possible. The existence and regulation of the topography-triggered osteogenic memory effect (TTOME) were carefully studied by directly activating the osteogenic differentiation of BMSCs or indirectly activating the osteoimmunomodulation between macrophages and BMSCs. The exploration of these scientific issues will help guide the design of biodegradable bone implants with micro/nano-structures in the future (Scheme 1).

2. Materials and methods

2.1. Fabrication and characterization of HA bioceramics with different topographies

HA powders were purchased from Kunshan Chinese Technology New Materials Co., Ltd. HA bioceramics with a smooth surface (S0), nanorod structure (S1), micropattern structure (S2) and micro/nano-hierarchical structure (S3) were fabricated using template combining with a hydrothermal method according to our previous study.[8] In short, the purchased HA powders were first screened using a 200-mesh nylon mesh screen before being mixed with 6 wt% polyvinyl alcohol (PVA), and then screened using a 200-mesh nylon mesh screen to remove the excess PVA binders. Subsequently, we prepared HA bioceramics with a micropattern structure (S2) by first placing 400-mesh nylon mesh sieves on the surface of a steel die, and then adding HA powders, pressing with a pressure of 12 MPa, and finally sintering them in air at 1100 °C for 5 h. HA bioceramics with a smooth structure (S0) were also obtained using the pressing method under the same conditions, without adding mesh sieves as templates.

Furthermore, HA bioceramics S0 and S2 were processed by hydrothermal treatment in solution with ethylenediamine tetraacetic acid disodium calcium (0.055 M) and $Na_3PO_4{\cdot}12H_2O$ (0.125 M) for 24 h at 120 °C to successfully obtain HA bioceramics with a nanorod structure (S1) and micro/nano-hierarchical structure (S3). For avoiding the possibility of residual ions affecting the biocompatibility of HA bioceramics after hydrothermal treatment, HA bioceramics were cleaned with deionized water for 3 days and the deionized water was exchanged 3–5 times once a day.

The surface morphologies of HA bioceramics were characterized using scanning electron microscopy (SEM, SU8220, HITACHI, Japan). The stereostructure and roughness of HA bioceramics were evaluated using a 3-dimensional (3D) laser microscope (LEXT: OLS4000, Olympus, Japan).

2.2. TTOME in the aspect of directly stimulating osteogenic differentiation of hBMSCs

Cells culture and seeding. HA bioceramics were first sterilized by moist heat sterilization at 121 °C for subsequent cell culture. hBMSCs (Cyagen Biosciences, America) were cultured in basal medium (Cyagen Biosciences, America) with 10% fetal bovine serum (Cyagen Biosciences, America) to the third passage (passage 3) for following study. BMSCs were seeded on HA bioceramics in cell culture plates, which was called the first stage of cell culture. After culturing for 1 day or 7 days at the first stage, hBMSCs cultured on HA bioceramics (S0–S3) were digested with trypsin, followed by being seeded in a new cell culture plate without bioceramics at the same cell density, respectively. The reinoculated cells were cultured for further cell assays, including cell proliferation, alkaline phosphatase activity and osteogenic gene expression. For a better explanation, hBMSCs cultured on S0–S3 samples at the first stage for 1 day were labeled as S0-1d, S1-1d, S2-1d and S3-1d, respectively, while hBMSCs cultured on S0–S3 samples at the first stage for 7 days were labeled as S0-7d, S1-7d, S2-7d and S3-7d, respectively.

Cell adhesion and proliferation. Before other experiments, we first evaluated the effect of bioceramic stimulation on cells at the first stage on the subsequent cell morphology. Specifically, hBMSCs were seeded on S0–S3 samples at the first stage for 2 days, then transferred to HA-free blank plates for further culture of 24 h. Finally, cell adhesion was observed using a confocal laser scanning microscope (CLSM, Leica, Germany). For the cell proliferation study, hBMSCs digested from S0–S3 bioceramics were reseeded in a new 48-well culture plate without HA bioceramics at a density of 8×10^3 cells per well. When the reinoculated cells were further cultured for 1, 3 and 7 days, cell proliferation was evaluated by measuring the viability of hBMSCs at each timepoint. Briefly, after the culture medium was removed, 300 μL mixture of basal medium containing cell counting kit-8 (cck-8, Beyotime, USA) at 10 : 1 ratio was added to each well and incubation for 2 h at 37 °C. Then, a microplate reader (Bio-TEk, USA) was used to measure optical density (OD) absorbance values at 450 nm for assessing cell activity. All experiments were performed in triplicate.

Alkaline phosphatase (ALP) activity. For assaying ALP activity, hBMSCs digested from S0–S3 bioceramics were reseeded in a new 24-well culture plate without HA bioceramics at a density of 2×10^4 cells per well. After cultivation for 7 days, the residual medium in the culture plate was removed and replaced with 400 μl lysis buffer (0.1% Triton X100). For enhancing the lysis effect, culture plates containing lysis buffer were placed at −20 °C for 10 min and then at 4 °C for 1 h. The obtained cell lysates were centrifuged and the supernatant was collected for the ALP assay, which was measured by determining the

transformation of *p*-nitrophenyl-phosphate (*p*NPP: Sigma, St Louis, USA) at 405 nm using a microplate reader (Bio-tek, USA). In addition, the total cell protein content in each well was also measured according to a BCA Protein Assay Kit (Beyotime, USA). Finally, ALP activity was normalized with total cell protein content, and all the experiments were presented in triplicate.

Real-time polymerase chain reaction (PCR) assay. For real-time PCR assay, hBMSCs digested from S0–S3 bioceramics were reseeded in a new 6-well culture plate without HA bioceramics at a density of 15×10^4 cells per well. After being cultured for 7 days, the total RNA was extracted from cells using Trizol reagent (Invitrogen, USA) and then reverse-transcribed into cDNA by PrimeScriptTM RT Master Mix (TaKaRa, China). The followed PCR reaction was performed using Ex Taq DNA polymerase (TaKaRa, China) and the related genes runt-related transcription factor 2 (Runx2), bone morphogenetic protein-2 (BMP2), alkaline phosphatase (ALP) and collagen 1 (COL1) were measured for evaluating the osteogenesis activity, while β-actin was taken as a house-keeping gene for normalization. In addition, gene connexin 43 (Cx43) was also analyzed for investigating cell–cell communication.

2.3. TTOME from the aspect of osteoimmunomodulation between RAW264.7 macrophages and hBMSCs

The osteoimmunomodulation ability of micro/nano-structures was firstly evaluated. Briefly, RAW264.7 cells were respectively seeded on HA samples in 6-well culture plates for 2 and 4 days at the first stage, and the supernatant of the culture medium was collected. The conditioned medium for culturing hBMSCs was further prepared by mixing the collected supernatant with fresh medium at the ratio of 2 : 1. hBMSCs were then seeded in blank 6-well culture plates with fresh medium for 12 h at a cell density of 30×10^4 cells per well, followed by replacement with the conditioned medium for another 4 days of culture. During this process, hBMSCs cultured in the conditioned medium which was obtained from RAW264.7 cells incubated with S0/S3 samples for 2 and 4 days at the first stage were marked as S0-2d, S3-2d, S0-4d, and S3-4d, respectively. Real-time PCR analysis was performed following the same procedure in the above section. The related osteogenic genes, including BMP2, OCN, Runx2, and COL1 were measured.

To further investigate the memory effect of the activated osteoimmunomodulation properties by micro/nano-structures. RAW264.7 cells were seeded on HA samples for 1, 3 and 5 days respectively at the first stage, followed by being transferred into a blank 6-well culture plate for an incubation of 3 days. Then, the supernatant was collected, and the conditioned medium for hBMSCs was prepared by mixing the collected supernatant with fresh medium at the ratio of 2 : 1. Subsequently, hBMSCs were seeded in 6-well culture plates (30×10^4 cells per well) following the same procedure as the above study. At the end of the culture time, the cells were determined for evaluating the osteogenic differentiation activity of hBMSCs cultured for 3 days. The expressions of osteogenesis-related genes, including BMP2, Runx2, OCN, and OPN were measured by real-time PCR according to the stimulation time (1, 3 and 5 days) of micro/nano-structures on RAW264.7 at the first stage before transferring into a blank culture plate, and were divided into the following groups, S0-1d, S3-1d, S0-3d, S3-3d, S0-5d, and S3-5d, respectively.

2.4. Statistical analysis

All the data were expressed as means ± standard deviation with one way ANOVA (SPSS, v.17.5, USA). The statistically significant difference between two groups was marked when $p < 0.05$.

3. Results and discussion

3.1. The surface morphologies of HA bioceramics

HA bioceramics with different surface structures were successfully fabricated (Fig. 1). As shown in SEM images (Fig. 1a), the sample S0 was considered as the control group, displaying smooth and dense crystals of 0.5–1.5 μm. The sample S1, by contrast, possessed the nanorods with the diameter of 50–70 nm, while the sample S2 had the micropatterns composed of concave structures (length of ~106 μm and width of ~25 μm) and convex structures (length of ~65 μm and width of ~15 μm). Moreover, both the micropattern and nanorod structures are present on the surface of the sample S3. Micro/nano-hierarchical structure has been proved to synergistically promote osteogenesis differentiation and suggests the potential application as surface topography of bone grafts for accelerating bone regeneration.

In addition, the stereo-structures of HA bioceramics with different topographies were observed by a 3D laser microscope (Fig. 1b), and the surface roughness of HA bioceramics was represented by the value of the parameter of arithmetical mean height (Sa), which were 0.11, 0.49, 4.21, and 7.31 μm in sample S1, sample S2, sample S3, and sample S4, respectively. This result corresponded to the SEM images as sample S0 had the smoothest surface, while sample S3 had the roughest surface because of the hybrid of micro- and nano-structures. According to the previous studies, our result also implied that the S3 sample could promote better cell attachment and osteogenic differentiation because of the rougher surface.[8]

3.2. TTOME from the aspect of directly stimulating osteogenic differentiation of hBMSCs

We first studied whether the stimulation of bioceramics (S0–S3) on cells would affect the viability or morphology of cells in

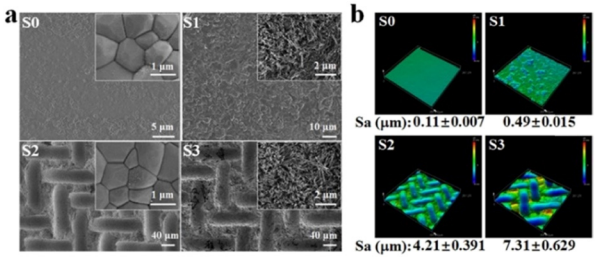

Fig. 1 (a) SEM images and (b) 3D images of HA bioceramics with the different surface structures: the smooth (S0), nanorod (S1), micropattern (S2) and micro/nanohierarchical surface (S3). The inset images in Fig. 1a represented the high magnification images of S0–S3, respectively.

subsequent culture. hBMSCs were seeded on S0–S3 bioceramics for 2 days at the first stage, and then respectively transferred into HA-free blank plate at the same cell density for a further culture of 24 h. Cells cytoskeletons were labeled for characterizing cells morphology as shown in Fig. 2. All groups of cells showed good spread, indicating that the stimulation from bioceramics at the first stage would not damage the subsequent cells morphology of hBMSCs. Compared to the cells stimulated by S0 at the first stage, the cells stimulated by S1–S3 with micro/nano-structures exhibited a better cell spread and more obvious pseudopodia at the later stage, especially the cells stimulated by S3, which seemed to indicate that topography-triggered cell adhesion could be remembered.

In our previous study, we found that HA bioceramics with micro- or nano-structures exhibited enhanced cell proliferation as compared with that of the flat sample, especially for the micro/nano-hierarchical structures.[8] Here, to evaluate whether the enhanced cell proliferation ability could be remembered, hBMSCs were first stimulated on S0–S3 bioceramics for 1 or 7 days, and then transferred into HA-free blank plate at the same cell density for the further culture of 1, 3, and 7 days, respectively. As shown in Fig. 3a–c, the enhanced cell proliferation ability activated by surface topographies could be indeed remembered since a similar tendency of hBMSC proliferation enhancement was exhibited in groups stimulated by S0–S3 as compared to the cell proliferation outcomes without the removal of HA bioceramics in our previous study,[8] in which the groups stimulated by S1 and S2 had a better effect as compared to the groups stimulated by S0, while the groups stimulated by S3 had the best cell proliferation at each timepoint. Such results confirmed that the topography-triggered cell behavior (such as the proliferation effect) could be remembered, designated as "memory effect" to reflect the sustained cell activation of micro- or nano-topographies even after the bone grafts are degraded. More interestingly, such topography-triggered cell proliferation effect could be regulated by the stimulation time as 7 days' stimulation significantly promoted more cell proliferation as compared to 1 day's stimulation in all corresponding groups (*e.g.*, S3-7d and S3-1d). Considering that different types of bioceramics, such as phosphate-based bioceramics and silicate-based bioceramics, have different degradation cycles. Such findings revealed the importance of the degradation rate of bone grafts with micro- or nano-topographies, which should be carefully regulated before being implanted.

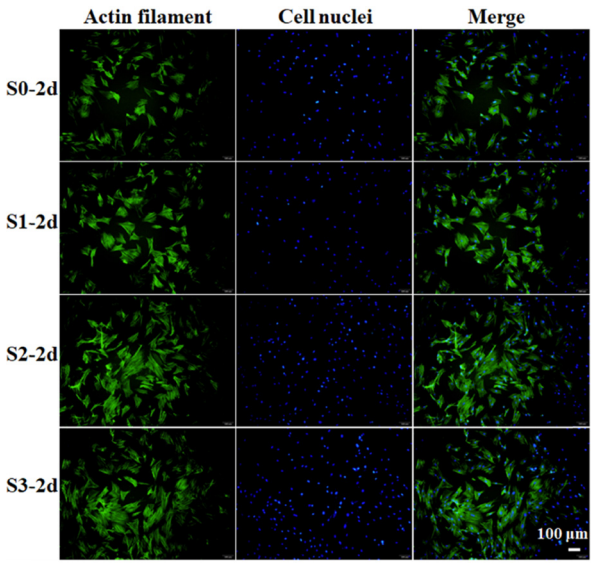

Fig. 2 Confocal microscopy images of hBMSCs incubated on S0–S3 for 2 days (S0-2d, S1-2d, S2-2d, S3-2d) and then transferred to HA-free blank plates for further culture of 24 h.

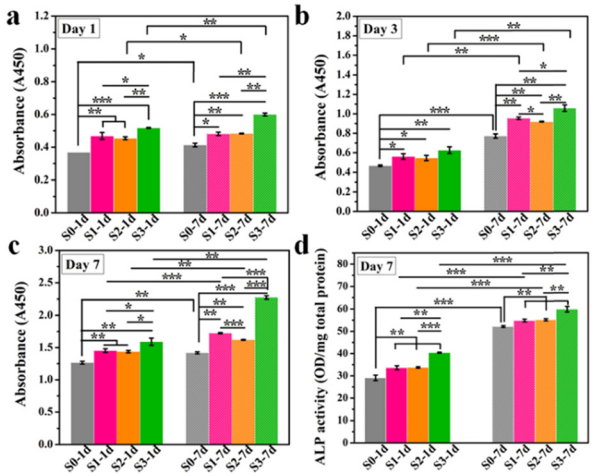

Fig. 3 The proliferation (a–c) and ALP activity (d) of hBMSCs incubated on S0–S3 for 1 day (S0-1d, S1-1d, S2-1d, S3-1d), or 7 days (S0-7d, S1-7d, S2-7d, S3-7d) and then transferred to HA-free blank plates for further culture. $*p < 0.05$, $**p < 0.01$, $***p < 0.001$.

To further evaluate the TTOME from the aspect of directly stimulating osteogenic differentiation of hBMSCs, the memory effect of the up-regulated ALP activity in hBMSCs activated by surface topographies was first confirmed since ALP was a typical biomarker for osteogenesis in the early stage. Similar to the cell proliferation study, hBMSCs were first stimulated on S0–S3 bioceramics for 1 or 7 days, and then transferred into a blank plate at the same cell density without HA bioceramics for another 7 days' incubation. As shown in Fig. 3d, hBMSCs on S1–S3 still expressed high ALP activity after 1 and 7 days of stimulation as compared to that on S0, which suggested that the topography-triggered early differentiation behavior of cells was persistent and eventually become a memory effect. And a similar tendency was displayed in the groups stimulated by S0–S3, in which S3 had the strongest ALP promotion, which was consistent with the outcomes of ALP expression without the withdrawal of HA bioceramics in our previous study.[8] Also, 7 days' stimulation significantly promoted the expression of ALP as compared to 1 day's stimulation in all corresponding groups (*e.g.*, S3-7d and S3-1d), which suggested that such topography-triggered memory effect of ALP activity could be regulated by the stimulation time.

Furthermore, the memory effect of the up-regulated osteogenic genes (BMP2, Runx2, ALP and COL1) in hBMSCs activated by surface topographies was revealed by a real-time qPCR

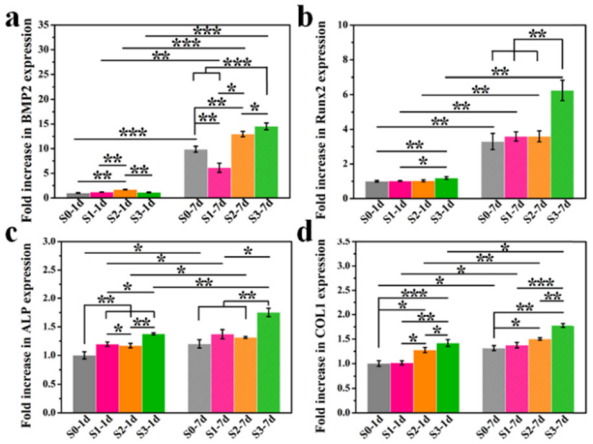

Fig. 4 Osteogenic genes expression of BMSCs cultured on S0–S3 for 1 day (marked as: S0-1d, S1-1d, S2-1d, S3-1d), 7 days (marked as: S0-7d, S1-7d, S2-7d, S3-7d) and then transferred to blank plates without HA bioceramics for a further culture of 7 days. *$p < 0.05$, **$p < 0.01$, ***$p < 0.001$.

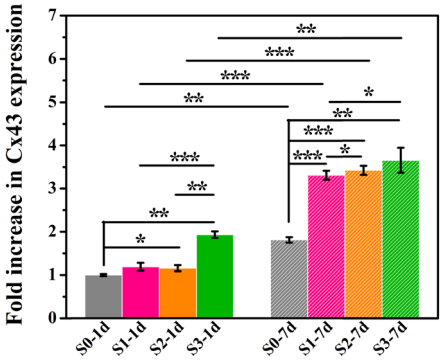

Fig. 5 Cx43 gene expression in hBMSCs cultured on S0–S3 for 1 day (marked as: S0-1d, S1-1d, S2-1d, S3-1d), 7 days (marked as: S0-7d, S1-7d, S2-7d, S3-7d) and then transferred to the blank culture plates for another 7 days. *$p < 0.05$, **$p < 0.01$, ***$p < 0.001$.

study. To guarantee the sufficient contents of proteins for testing, hBMSCs were first stimulated on S0–S3 bioceramics for 1 or 7 days, and then transferred into a blank 6-well plate at the same cell density without HA bioceramics for another 7 days' incubation. As shown in Fig. 4, the cells that underwent topographic early stimulation still expressed a high level of osteogenic differentiation after removing the stimulation of micro/nano-structures. Cells stimulated by S1–S3 bioceramics for either 1 day or 7 days showed stronger expression of osteogenic genes than those stimulated by the S0 bioceramic, which suggested that the memory effect of topography-triggered osteogenic differentiation could be sustained. In particular, the micro/nano-hierarchical structure (S3) still played the most significant role in continuously activating the expression of osteogenic genes as presented in our previous study.[8] It is worth mentioning that the topography-triggered memory effect could be easily regulated by the length of topographic stimulation. Magically, Ma *et al.*[19] also reported a theory of nanotopographic memory of small extracellular vesicles for bone regeneration. They found that small extracellular vesicles extracted from hBMSCs which were stimulated by nanotopography could copy the pro-osteogenesis effect from the nanotopography to enhance bone regeneration, which seemed to be consistent with our study. These results also indicated that topography-triggered memory effect deserved to be further studied.

Furthermore, the gene expression of Cx43 was assessed, which was regarded as a major connexin for cell–cell communication.[20,21] Our previous study has proved that micro/nano-structures could up-regulating the expression of Cx43.[8] Here, as shown in Fig. 5, cells that underwent the stimulation of micro/nano-structures (S1–S3) at the early stage expressed higher amount of Cx43 in subsequent HA-free cultures, as compared to cells stimulated by smooth surface (S0), which indicated that the topography-triggered memory effect on cell–cell communication could be retained. In addition, the persistence of micro/nano-structure activation in the memory effect of cellular behaviors was further investigated. Cells cultured on micro/nano-structures for 7 days showed a higher Cx43 protein expression than those incubated for only 1 day, which suggested that the stimulation time of micro/nano-structures could regulate the memory effect of cell behaviors. Undoubtedly, the early stimulation from micro/nano-hierarchical structure was still seen to be the strongest promoter in the expression of Cx43 *via* triggering the memory effect of hBMSCs. Our previous study has also indicated that Cx43 mediated cell–cell communication could promote osteogenic differentiation by interacting with BMP2 signaling pathways.[8] Considering that Cx43 mediated cell–cell communication played a crucial role in bone regeneration, topography-triggered cell–cell communication may also have a memory function, and possessed the potential to regulate osteogenic differentiation by copying stimulation information from the micro/nano-structures.

Previous studies have demonstrated that the micro/nano-structures could promote the osteogenic differentiation of BMSCs.[22–24] Our results preliminarily indicated that the cell behaviors (*e.g.*, osteogenic differentiation and cell–cell communication) which have been activated by micro- or nano-structures were still maintained even when stimulation of surface structures disappeared. More importantly, such TTOME might be manipulated by the stimulation time, which offers a potential theoretical basis for the design of bone implants with an optimal degradation rate of topographies.

3.3. TTOME from the aspect of osteoimmunomodulation between RAW264.7 macrophages and hBMSCs

Previous studies have proved that the immune response produced by implanted biomaterials into bone defect sites would influence the tissue regeneration process.[25,26] As a predominant immune cell, macrophages could be polarized towards different phenotypes and further modulate the osteogenic differentiation of BMSCs. In particular, biomaterials with micro/nano-structures could stimulate macrophages towards phenotype M2 and further enhanced tissue regeneration.[18,27]

The effect of the immune response of RAW264.7 cells stimulated by micro/nano-structures for different days on

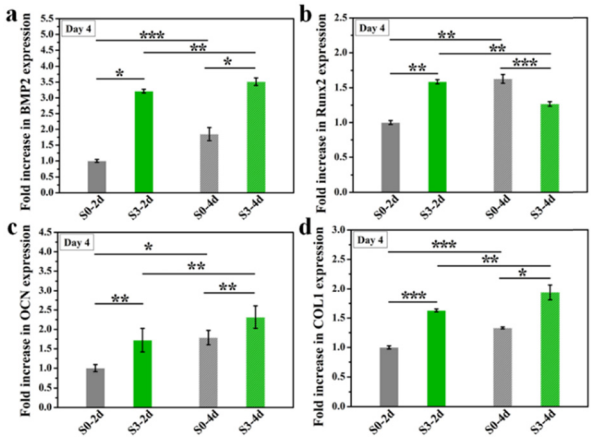

Fig. 6 The osteogenic gene expression of hBMSCs cultured in RAW 264.7 cells conditioned medium which were stimulated by micro/nano-structures for 2 or 4 days. *$p < 0.05$, **$p < 0.01$, ***$p < 0.001$.

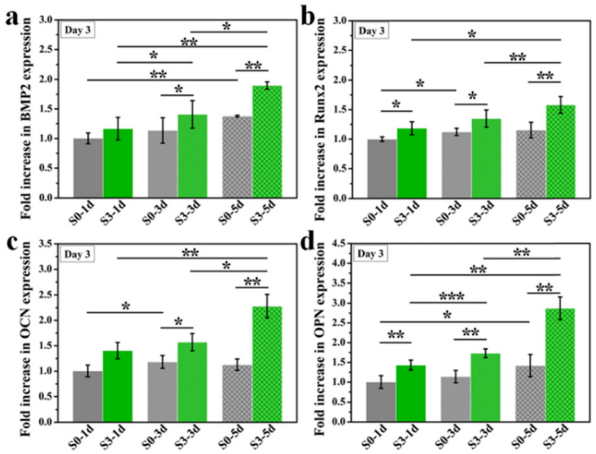

Fig. 7 The osteogenic gene expression of hBMSCs cultured in conditioned medium of RAW 264.7 cells which were cultured for 3 days after the stimulation of micro/nano-structures (S0, S3) for 1 day (marked as: S0-1d, S3-1d), 3 days (marked as: S0-3d, S3-3d), and 5 days (marked as: S0-5d, S3-5d), respectively. *$p < 0.05$, **$p < 0.01$, ***$p < 0.001$.

osteogenic differentiation of hBMSCs was firstly examined. Here, only micro/nano-hierarchical structure (S3) and the control group (S0) were selected for further cell experiments since sample S3 exhibited the strongest promotion of osteogenic differentiation as compared to samples with the nano-structure (S1) alone or the micro-structure (S2) alone. As shown in Fig. 6, sample S3 had better regulation of the osteoimmune microenvironment as higher osteogenic genes (BMP2, OCN, COL1 and Runx2) were expressed in hBMSCs after being cultured with the conditioned medium collected from RAW264.7 macrophages stimulated by sample S3 as compared to sample S0. Also, an enhanced osteoimmunomodulation ability was observed in both sample S0 and sample S3 when the stimulation time was prolonged from 2 days to 4 days, indicating the importance of maintaining bone grafts with suitable topographies for the osteoimmunomodulation.

Furthermore, we wondered if such topography-triggered osteoimmunomodulation properties could be remembered after the removal of HA bioceramics. Therefore, we cultured RAW264.7 macrophages on sample S0 and S3 for 1, 3, or 5 days, respectively, and then transferred them into a HA-free blank plate at the same cell density for another 3 days' incubation. Sequentially, the hBMSCs were cultured for 3 days with the conditioned medium collected from the above samples. As shown in Fig. 7, the TTOME in the aspect of osteoimmunomodulation between RAW264.7 macrophages and hBMSCs was confirmed due to similar trends as compared to the results in Fig. 7. In a nutshell, the micro/nano-hierarchical structures (S3) prompted higher osteogenic gene (BMP2, OCN, COL1 and Runx2) expression in hBMSCs through the osteoimmunomodulation as compared to the plane structures (S0), and this regulatory effect could be remembered even after the HA bioceramics were removed. In addition, the prolonged stimulation time on HA bioceramics would significantly improve the memory effect, especially for sample S3-5d, which had the best osteoimmunomodulatory effect. Our study revealed that the topography-activated osteoimmune microenvironment could be remembered and regulated, suggesting that the biomaterial with a rational surface structure and degradation rate might achieve a long-term favourable immune microenvironment, and ultimately affect the regeneration results.

4. Conclusions

Considering the importance of micro/nano-structured surface topography on osteogenesis and the inevitable degradation of these topographies *in vivo*, it is of great significance to deeply study bone regeneration after the degradation of the surface topography. In this study, for mimicking cell behaviors (*e.g.*, proliferation, osteogenic differentiation) before and after degradation, hBMSCs and RAW 264.7 macrophages were cultured on HA bioceramics with different surface structures for a certain time, and then transferred to new HA-free culture plates at the same cell density for further culture to explore the potential effect of surface degeneration. Our results confirmed the existence and tailorability of TTOME, which depended on the surface structures and simulation time, not only for direct promotion of osteogenic differentiation of hBMSCs but also for the indirect osteoimmunomodulation between RAW264.7 macrophages and hBMSCs. This study could provide a potential theoretical basis to prepare biodegradable biomaterials with micro- or nano-structures for bone regeneration.

Author contributions

Jiang Chang and Cancan Zhao designed the present work. Jiang Chang and Xudong Wang supervised the work and commented on it. Cancan Zhao, Qun Lou, and Jiashu Yan performed experiments. Cancan Zhao and Chen Yang analyzed the data and wrote the manuscript. All the authors contributed to the discussion during the whole work.

Conflicts of interest

There are no conflicts to declare.

Acknowledgements

This study is funded by the National Natural Science Foundation of China (82001006, 32271386, and 31900945), the Program of Shanghai Academic/Technology Research Leader (20XD1433100), the Zhejiang Traditional Chinese Medicine Scientific Research Fund Project (2022ZB342), the seed grants from the Wenzhou Institute, University of Chinese Academy of Sciences (WIUCASQD2020013 and WIUCASQD2021030), and the funding from the First Affiliated Hospital of Wenzhou Medical University. Also, we thank the Scientific Research Center of Wenzhou Medical University for consultation and instrument availability that supported this work.

Notes and references

1 D. Arcos and M. Vallet-Regi, *J. Mater. Chem. B*, 2020, **8**, 1781–1800.
2 T. Li, J. Chang, Y. Zhu and C. Wu, *Adv. Healthcare Mater.*, 2020, **9**, e2000208.
3 T. Li, D. Zhai, B. Ma, J. Xue, P. Zhao, J. Chang, M. Gelinsky and C. Wu, *Adv. Sci.*, 2019, **6**, 1901146.
4 J. Zhang, D. Tong, H. Song, R. Ruan, Y. Sun, Y. Lin, J. Wang, L. Hou, J. Dai, J. Ding and H. Yang, *Adv. Mater.*, 2022, **34**, e2202044.
5 S. Elsharkawy, M. Al-Jawad, M. F. Pantano, E. Tejeda-Montes, K. Mehta, H. Jamal, S. Agarwal, K. Shuturminska, A. Rice, N. V. Tarakina, R. M. Wilson, A. J. Bushby, M. Alonso, J. C. Rodriguez-Cabello, E. Barbieri, A. Del Rio Hernandez, M. M. Stevens, N. M. Pugno, P. Anderson and A. Mata, *Nat. Commun.*, 2018, **9**, 2145.
6 C. Q. Zhang, D. A. McAdams and J. C. Grunlan, *Adv. Mater.*, 2016, **28**, 6292–6321.
7 T. Li, F. Han, J. Xue, H. Ma, Y. Wang, M. Zhuang, D. Ren, L. Wang, J. Chang and C. Wu, *Appl. Mater. Today*, 2021, **25**, 101194.
8 C. Zhao, X. Wang, L. Gao, L. Jing, Q. Zhou and J. Chang, *Acta Biomater.*, 2018, **73**, 509–521.
9 C. Zhao, L. Xia, D. Zhai, N. Zhang, J. Liu, B. Fang, J. Chang and K. Lin, *J. Mater. Chem. B*, 2015, **3**, 968–976.
10 L. Ma, G. Li, J. Lei, Y. Song, X. Feng, L. Tan, R. Luo, Z. Liao, Y. Shi, W. Zhang, X. Liu, W. Sheng, S. Wu and C. Yang, *ACS Nano*, 2022, **16**, 415–430.
11 R. Sridharan, A. R. Cameron, D. J. Kelly, C. J. Kearney and F. J. O'Brien, *Mater. Today*, 2015, **18**, 313–325.
12 K. L. Spiller and T. J. Koh, *Adv. Drug Delivery Rev.*, 2017, **122**, 74–83.
13 Q. Huang, Z. Ouyang, Y. Tan, H. Wu and Y. Liu, *Acta Biomater.*, 2019, **100**, 415–426.
14 Z. Chen, A. Bachhuka, S. Han, F. Wei, S. Lu, R. M. Visalakshan, K. Vasilev and Y. Xiao, *ACS Nano*, 2017, **11**, 4494–4506.
15 J. M. Sadowska, F. Wei, J. Guo, J. Guillem-Marti, M. P. Ginebra and Y. Xiao, *Biomaterials*, 2018, **181**, 318–332.
16 Y. He, M. Yao, J. Zhou, J. Xie, C. Liang, D. Yin, S. Huang, Y. Zhang, F. Peng and S. Cheng, *Regener. Biomater.*, 2022, **9**, rbac027.
17 D. Yu, S. Guo, M. Yu, W. Liu, X. Li, D. Chen, B. Li, Z. Guo and Y. Han, *Bioact. Mater.*, 2022, **10**, 323–334.
18 C. Yang, C. Zhao, X. Wang, M. Shi, Y. Zhu, L. Jing, C. Wu and J. Chang, *Nanoscale*, 2019, **11**, 17699–17708.
19 L. Ma, W. Ke, Z. Liao, X. Feng, J. Lei, K. Wang, B. Wang, G. Li, R. Luo, Y. Shi, W. Zhang, Y. Song, W. Sheng and C. Yang, *Bioact. Mater.*, 2022, **17**, 425–438.
20 R. A. Rossello, Z. Wang, E. Kizana, P. H. Krebsbach and D. H. Kohn, *Proc. Natl. Acad. Sci. U. S. A.*, 2009, **106**, 13219–13224.
21 A. Tirosh, G. Tuncman, E. S. Calay, M. Rathaus, I. Ron, A. Tirosh, A. Yalcin, Y. G. Lee, R. Livne, S. Ron, N. Minsky, A. P. Arruda and G. S. Hotamisligil, *Cell Metab.*, 2021, **33**, 319–333.
22 T. Li, B. Ma, J. Xue, D. Zhai, P. Zhao, J. Chang and C. Wu, *Adv. Healthcare Mater.*, 2020, **9**, 1901211.
23 T. Li, D. Zhai, B. Ma, J. Xue, P. Zhao, J. Chang, M. Gelinsky and C. Wu, *Adv. Sci.*, 2019, **6**, 1901146.
24 C. Yang, Z. Huan, X. Wang, C. Wu and J. Chang, *ACS Biomater. Sci. Eng.*, 2018, **4**, 608–616.
25 D. Venugopal, S. Vishwakarma, I. Kaur and S. Samavedi, *Acta Biomater.*, 2022, DOI: **10.1016/j.actbio.2022.06.004**.
26 D. R. Griffin, M. M. Archang, C.-H. Kuan, W. M. Weaver, J. S. Weinstein, A. C. Feng, A. Ruccia, E. Sideris, V. Ragkousis, J. Koh, M. V. Plikus, D. Di Carlo, T. Segura and P. O. Scumpia, *Nat. Mater.*, 2021, **20**, 560–569.
27 W. Zhang, H. Lopez, L. Boselli, P. Bigini, A. Perez-Potti, Z. Xie, V. Castagnola, Q. Cai, C. P. Silveira, J. M. de Araujo, L. Talamini, N. Panini, G. Ristagno, M. B. Violatto, S. Devineau, M. P. Monopoli, M. Salmona, V. A. Giannone, S. Lara, K. A. Dawson and Y. Yan, *ACS Nano*, 2022, **16**, 1547–1559.

